Inorganic Chemistry, 2020, 59, 15, 10482–10491, https://doi.org/10.1021/acs.inorgchem.0c00794

Striking Increase of Hole Mobility Upon Metal Coordination to Triphenylene-Schiff-Base Semiconducting Multicolumnar Mesophases.

Estela de Domingo,[a] César L. Folcia,[b] Josu Ortega,[c] Jesús Etxebarria,[b] Roberto Termine,[d] Attilio Golemme,[d] Silverio Coco,[a] and Pablo Espinet.*[a]*

[a] *IU CINQUIMA/Química Inorgánica, Facultad de Ciencias, Universidad de Valladolid, 47071 Valladolid, Castilla y León, Spain.* [b] *Condensed Matter Physics, University of the Basque Country, UPV/EHU, 48080 Bilbao, Spain.* [c] *Applied Physics II, University of the Basque Country, UPV/EHU, 48080 Bilbao, Spain.* [d] *LASCAMM CR-INSTM, CNR-Nanotec, Dipartimento di Fisica, Università della Calabria, 87036 Rende, Italy.*

ABSTRACT: This paper reports the synthesis, liquid crystal behavior, and charge-transport properties in the mesophase of triphenylene Schiff-bases and their copper(II), nickel(II) and oxovanadium(IV) complexes. The thermal and electronic properties of the Schiff-bases are modulated by coordination to the corresponding metal moieties, which have the ability to self-assemble into linear structures and help the alignment of the triphenylene columns. This produces two kinds of electronically non-connected columnar regions, one purely organic and one more inorganic. The most remarkable effect is a striking charge mobility enhancement in the metal containing mesophases, due to the contribution of the more inorganic columns: compared to values of hole mobility along the columnar stacking for the purely organic columnar mesophases, in the order of 10^{-7} cm^2 V^{-1} s^{-1}, these values jump to 1-10 cm^2 V^{-1} s^{-1} in these hybrid inorganic/organic columnar materials.

Supporting Information Placeholder

INTRODUCTION

Substituted triphenylene derivatives that give rise to columnar mesophases have been systematically investigated in the last decades and are nowadays a classic field in the area of liquid crystals.[1-4] Many studies show that these liquid crystals (LC) display interesting physical and chemical properties making them suitable candidates for several applications such as electrophotography,[5] electronics and optoelectronics,[6] LEDs,[7] or chemical sensing.[8] They have been also studied as materials for surface modification,[9] as stabilizers of nanoparticles,[10,11] as fluorescent ferroelectric materials,[12] and even for birefringent films that improve the viewing angle of liquid crystal displays.[13]

There are many reports where electron-withdrawing or donating side groups are covalently bonded directly to the triphenylene core: nitro and amino groups,[14-17] cyano group,[18] halides,[19,20] alkyl/alkoxy fragments,[21,22] or organometallic moieties.[23-29] In all of them the π-π interactions, critical for the columnar stacking, are sensitive to the substituents. There are also reports where the triphenylene is functionalized at the end of one of the alkoxy substituents,[30] so that the triphenylene core and the functional group are far apart and electronically disconnected. This case can favor the formation of mesophases with segregated columns of different nature,[31-33] and interesting mesophases with ambipolar charge transport properties,[34-37] or with efficient photocurrent generation.[38,39]

In previous studies we have shown that in the lack of attractive intermetallic interactions between the metallic moieties, self-organization of the triphenylene discs controls the formation of columnar mesophases, giving rise to well-defined organic zones that support the attached metallic moieties.[40,41] However, using metal-containing moieties prone to induce metal···metal intermolecular interactions, dual well-ordered columnar and highly stabilized phosphorescent mesophases were obtained.[42] Numerous studies have suggested that metallophilic interactions are key to the induction of mesomorphism in platinum(II) materials,[43-46] as well as in some gold compounds.[47,48] For conventional isocyano benzoquinolate platinum complexes that give rise to columnar mesophases, the benzoquinolate platinum fragments are connected by Pt···Pt interactions, their liquid crystalline version shows high one-dimensional charge mobility along the columnar stacking. Unfortunately, the free benzoquinol ligand was not liquid crystal and a direct comparison of charge mobility in mesophase between the organic ligand and its metal complexes was not possible.[49]

Here we focus our attention to Salen-type metal complexes, a well studied source of metallomesogens.[50-52] They are known to self-assemble into one-dimensional structures via M···M,[53,54] M···O,[55,56] or M···N interactions.[54] In this work we report uncommon mesomorphic triphenylene-Schiff-base complexes of copper(II), nickel(II), and oxovanadium(IV), which display much higher hole mobility along the columnar stacking of their mesophases, than their organic precursors. The hole mobility was measured by the space-charge-limited current (SCLC) method.

RESULTS AND DISCUSSION

Synthesis and Characterization

The syntheses of the ligands and their complexes are sketched in Scheme 1. The starting reactive 4-substituted-2-hydroxybenzaldehyde was obtained using modified literature

methods.[57,58] The new Schiff bases **1a-1c** were synthesized by condensation of the 4-substituted-2-hydroxybenzaldehyde with the respective diamine. The metal complexes were prepared by reacting the Schiff bases with the corresponding metal salt.[57,59] Similar conventional complexes without the triphenylene group (reasonable models to **2a-2c**, **3a-3c** and **4a-4c**) are square planar for Ni,[53,54] square-planar or distorted square planar for Cu,[54,60] and square pyramidal for oxovanadium.[54]

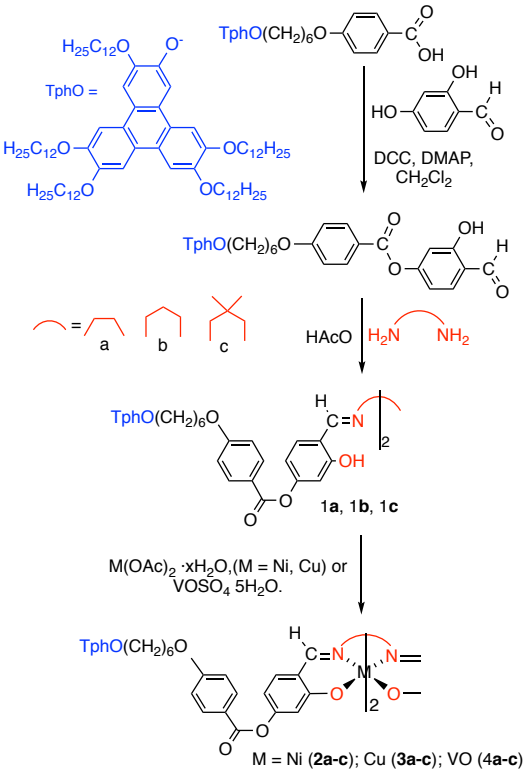

Scheme 1. Synthesis of Schiff bases (**1**) and their nickel(II) (**2**), copper(II) (**3**), and oxovanadium(IV) (**4**) complexes**.**

The IR spectra of the metal complexes display typical ν(C=N) bands from the imine groups in the range 1615–1618 cm^{-1}.[61] In addition, the vanadyl complexes display ν(V=O) at 983, 857, and 871 cm^{-1}, respectively for **4a**, **4b**, and **4c**. These V=O bands report on the strength of intermolecular interactions via vanadyl.[55,56] Lower ν(V=O) indicate stronger intermolecular interactions. In **4a** this frequency supports essentially no V=O→V=O interactions, but in **4b** and **4c** these interactions are observed in the solid state and in the mesomorphic state (stronger in **4b** than in **4c**), giving rise to linear →V=O→V=O→ chain structures.

The Ni^{II} complexes show well-resolved ^1H and $^{13}C\{^1H\}$ NMR spectra, consistent with square-planar diamagnetic molecules. In contrast, the copper and vanadyl complexes are paramagnetic molecules and display very broad ^1H NMR signals.

The UV-Vis absorption spectra of both the ligands and their complexes in CH_2Cl_2 solution, plotted in Figure 1 for Salen compounds (details in Supporting Information), were recorded at high dilution (10^{-5} M) to avoid autoabsorption phenomena induced by molecular aggregation. The electronic absorption spectra of the free ligands are all very similar, displaying a very structured spectral pattern with intense absorption bands typical of 2,3,6,7,10,11-hexaalkoxytriphenylenes.[62,63] For the metal complexes, the electronic spectra show, in addition, one low intensity broad absorption band in the range 406-613 nm, corresponding to the metal moiety (Ni,[64,60] Cu,[65] VO[61]).

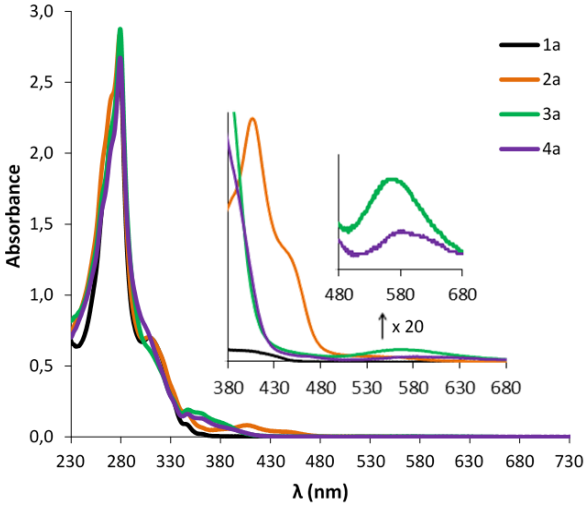

Figure 1. UV-Visible spectra of the free ligand Salen (**1a**) and the complexes [(Salen)Ni] (**2a**), [(Salen)Cu] (**3a**), and [(Salen)VO] (**4a**), in dichloromethane (10^{-5} M) at 298 K. The magnified region is from 10^{-4} M solutions.

Thermal behavior and self-organization properties

The mesomorphic properties have been studied using polarized optical microscopy (POM), differential scanning calorimetry (DSC), and small-angle X-ray scattering (SAXS). All complexes display good thermal stability. The optical, thermal and thermodynamic data are collected in Table 1.

Table 1. Optical, thermal, and thermodynamic data for the Schiff bases and their metal complexes.

[a] Cr, crystal phase; G, glass phase; Col_h, hexagonal columnar

Compound	Transition[a]	Temp.[b] (°C)	ΔH[b] ($kJmol^{-1}$)
Salen (1a)	Cr→Col_h Col_h →I	54 78	63.6 18.7
Ni (2a)	Cr→N_{Col} N_{Col}→I	26 103	11.8 18.7
Cu (3a)	G→Col_r Col_r→I	27 88	 8.5
VO (4a)	G→M M→I	26 104	 3.8
Salpn (1b)	Cr→I	36	37.7[c]
Ni (2b)	Cr→Col_r Col_r →I	23 99	8.1 21.1
Cu (3b)	G→ Col_r Col_r →I	37 77	 9.6
VO(4b)	Cr→ Col_h Col_h →I	27 144	15.1 18.1
Me_2Salpn (1c)	Cr→I	35	57.2[c]
Ni (2c)	G→I	48	
Cu (3c)	Cr→I	77	15.7
VO (4c)	Cr→ Col_r Col_r →I	29 109	22.8 22.7

mesophase; Col_r, rectangular columnar mesophase; $N_{Col:}$, nematic columnar mesophase; I, isotropic liquid; M: unidentified mesophase. [b] Data collected from the second heating DSC cycle. [c] Combined enthalpies. The transition temperatures are given as peak onsets.

For the free Schiff bases, only Salen (**1a**) displays liquid crystal behavior. All the metal complexes with Salen (**2a**, **3a**, **4a**) or Salpn (**2b**, **3b**, **4b**) show enantiotropic mesomorphism at temperatures close to ambient. In contrast, for the Me_2Salpn derivatives only the vanadyl complex (**4c**) displays liquid crystal behavior. Apparently the steric demand of the geminal methyls is detrimental for efficient intermolecular interactions, but reinforcement with V=O→V=O interactions restores the ability to form a mesophase. On cooling, most of the compounds do not display a crystallization process, but a glass transition or a partial crystallization, is frequently observed.

Representative microphotographs are shown in Figure 2. The textures observed by POM on cooling from the isotropic liquid are fluid and birefringent, but rather unspecific in most cases, although **4b** displays a beautiful pseudo-focal conic texture suggesting a columnar mesophase (Figure 2c), which was confirmed in the diffraction studies.

The quite regular variation in thermal properties of the mesomorphic families can be summarized as follows: a) all the mesomorphic complexes melt at temperatures lower than the free ligand, within the short temperature range 23-29 °C; b) the clearing temperatures, as well as the mesophase ranges decreases regularly in the order VO > Ni > Cu in each series.

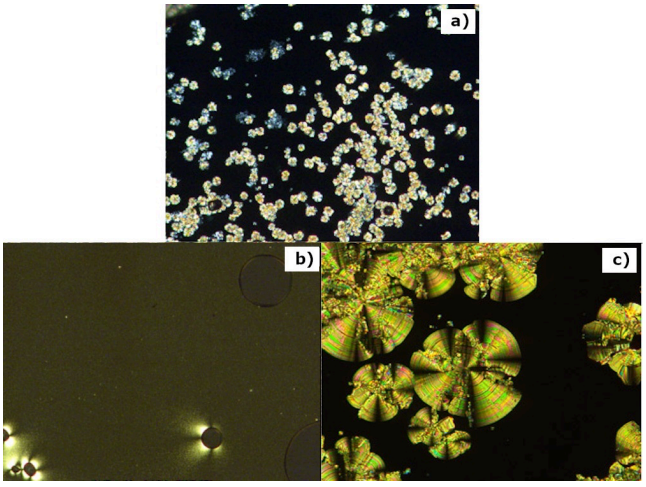

Figure 2. Optical polarizing microscopy photographs (x100, crossed polarizers) on cooling from the isotropic phase of: a) Salen base (**1a**), Col_h at 65 °C; b) Ni(Salen) complex (**2a**), N_{Col} at 60 °C; and c) vanadyl(Salpn) complex (**4b**), Col_h at 130 °C.

The rationale of the mesomorphic behavior of materials is not a simple matter, but for similar molecular systems it can be qualitatively approached on the basis of the simple enthalpy/entropy considerations.[49] The formation of a mesophase by molecular self-association occurs when the enthalpy of the process compensates for the unfavorable entropic contribution of association. For the molecules under consideration, similar in shape if they use the same ligand, and all leading to columnar-like mesophases, we can suppose that the entropic contribution should be fairly similar in all the complexes. For the enthalpic contribution two interactions have to be considered: the π-π triphenylene-triphenylene stacking, and the metal-moieties interactions. Regarding the former, the triphenylenes are far away and electronically isolated from the metals. It looks plausible that their enthalpic contributions should be fairly similar, whether without or with different metals. Hence, we can expect the mesophase ranges and temperatures to be roughly dependent on the strength of interactions between metal moieties. These can be very different, as suggested by crystal packing data of analogous but simpler metal complexes without triphenylene substituents. These complexes often show molecules packed in antiparallel disposition giving rise to discrete dimers, in the case of nickel[53] and copper Salen compounds (models for **2a** and **3a**),[66] or to infinite one-dimensional chains in the rest.[53,55,66] The formation of multiple intermolecular N···H_{aryl} and O···H_{aryl} interactions contributes in all cases to the stacking of the metal moieties, and oxygen-metal or other interactions (depending on the metal) also contribute to this ordered arrangement.

The model complex of **2a** displays weak Ni···Ni interactions, through discrete dimers or one-dimensional chains (models of **2b**),[53] whereas the copper complexes display either linear chain structures with no specific interactions of the metals (in Salpn derivative models of **3b**), or discrete dimers through two weak axial M···O interactions (in conventional Salen complexes model of **3a**) (Figure 3).[54,66] In addition, in the molecular packing of the nickel complexes the intermolecular distances are shorter than in those of the copper derivatives, both in the dimers and in the chain structures. This suggests stronger intermolecular interactions in the nickel complexes than in the copper analogues.

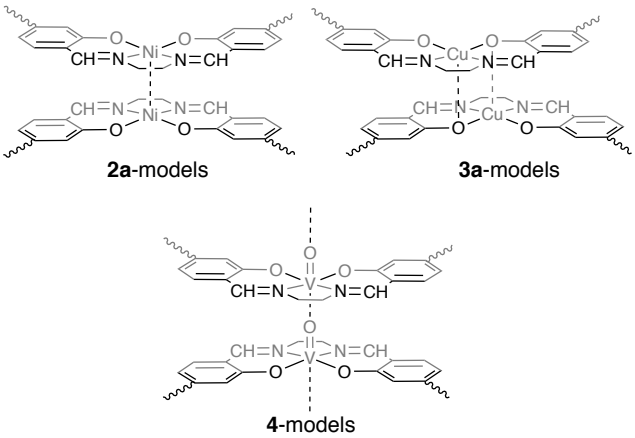

Figure 3. Schematic representation of common molecular packings of Salen Ni, Cu and VO complexes.

The oxovanadium derivatives show the already commented head-to-tail alignment of vanadyl groups in linear chain structures (→V=O→V=O→).[55,67,68] According to the frequency of the V=O stretching mode above discussed, the strength of the O→V interaction decreases in the order **4b** > **4c** >> **4a**; in **4a** this interaction is practically lost. Consistent with this analysis the clearing temperature and the mesophase range should increase in the order: Shiff-base < Cu < Ni < VO, as observed. It is worth noting that in simple monomeric *trans*-bis-salicylaldimine complexes, where the mesomorphic behavior

depends on the planarity of the chelate core structure, the thermal stability of the mesophases decreases in the order Ni > Cu > VO.[52] The different with our complexes is that in our salen-type metal complexes the *cis*-N_2O_2 coordination creates a net molecular dipole, but in the *trans*-bis-salicylaldimine complexes the dipolar moments of the coordinated bonds cancel each other. Thus, similar behavior is not necessarily expected.

Small-angle X-ray Scattering (SAXS) Studies.

X-ray scattering measurements were performed to study the structural properties of these mesophases. In the small-angle region material **2a** shows two broad diffuse reflections at 2θ = 1.74° and 2θ = 3.95°, supporting a nematic phase consistent with POM observations (Figure 2b). The characteristic distances (55 Å and 23 Å) appear also, with only small variations, in the isotropic phases of all the other materials, suggesting that they are related to the molecular dimensions.

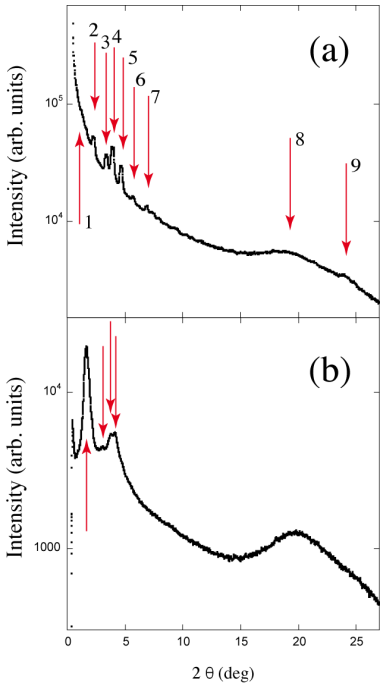

Figure 4. (a) Small-angle reflections for **4b** at 100 °C (peaks Nos. 1-7). Only peaks 2, 3, 4, and 5 were considered for the calculation of the charge-density maps. At wide angles peak 8 is the diffuse halo and peak 9 is connected with the stacking distance of the columns in the mesophase. (b) Diffraction diagram of material **3b** at 70 °C. Red arrows indicate the observed reflections.

The diffraction diagrams of the rest of the compounds are typical of columnar phases. The diagrams present systematically a diffuse halo at wide Bragg angles $2\theta \approx 20°$, indicating a certain degree of fluidity of the phases (see two representative examples in Fig. 4). The distance (about 4.5 Å) corresponds to the width of the alkyl chains that fill the empty space. This halo could indicate absence of crystalline ordering along the column axes, meaning the material is a columnar liquid-crystal phase. The two-dimensional columnar order observed and the fluidity of these materials, similar to others in our previous related papers, lead us to assign the nomenclature of the columnar mesophases in Table 1.

At even wider angles $2\theta \approx 24°$, a sharper reflection is also visible in most cases (see peak 9 in Fig. 4a). This spacing (about 3.6 Å) is connected to the stacking distance between triphenylene groups, which presumably transmit their columnar organization to the rest of the molecular fragments, finally giving rise to the overall columnar mesophase. This reflection can also be appreciated in the nematic material **2a,** suggesting that in this case the objects that present nematic ordering are composed of several molecules with columnar-like packing.

The peak positions of the X-ray reflections together with their relative intensities are given in Table 2 for the different materials, except for the free ligand **1a** and for **4b**, which will be discussed separately. The diffraction diagrams could be indexed assuming a rectangular columnar structure. The low-angle X-ray diagrams for materials **2a**, **3a**, **2b**, and **4c** are gathered in Fig. S51. In these structures the calculated mass density was close to ρ = 1 g/cm^3 when taking an integer number of molecules per unit cell (Z) and an intracolumnar stacking distance h = 3.6 Å.

The other two materials (**1a**, and **4b**) had completely different diffraction patterns, and were successfully indexed according to a hexagonal lattice (Tables 3 and 4). For the sake of completeness the low-angle X-ray diagram for the free ligand **1a** can also be found in the S.I. (Fig. S52).

Table 2. X-ray scattering results of compounds **2a**, **3a**, **2b**, **3b**, and **4c.** The cell parameters depend slightly on the temperature. (Z = number of molecules per unit cell).

Compd.	T (°C)	Cell parameters	Peak position 2θ (°)/Miller ind.	Normaliz. intensity
2a	60	Nematic	1.74 Diffuse 3.95 Diffuse	1 0.18
3a	65	a = 85.7 Å b = 73.8 Å Z = 4	1.56/(11) 2.65/(12) 3.69/(13) 4.01/(40)	1 0.01 0.07 0.07
2b	70	a = 84.5 Å b = 54.9 Å Z = 3	1.94/(11) 3.19/(02) 3.86/(22) 4.19/(40) 4.90/(03)	1 0.08 0.11 0.18 0.04
3b	70	a = 94.3Å b = 63.9 Å Z = 4	1.66/(11) 3.05/(31) 3.74/(40) 4.11/(03)	1 0.03 0.12 0.14
4c	85	a = 87.3 Å b = 82.6 Å Z = 4	1.46/(11) 2.00/(20) 2.89/(22) 3.85/(23) 4.03/(40) 4.73/(24) 5.37/(05)	1 0.15 0.02 0.27 0.35 0.03 0.02

Table 3. Small-angle reflections for the free ligand (**1a**). Peaks are indexed according to a hexagonal lattice with cell parameter a = 58.6 Å. All combinations of signs in the Miller indices are possible and correspond to symmetry equivalent reflections.

Norma-liz. Inten-sity	2θ (°) (exp.)	2θ (°) (calcd.)	Ratio of spacings d(10)/d(*hk*)	Miller indices (*hk*)
1	1.74	1.74	1	± (10) ± (01) ± (1-1)
0.36	3.01	3.01	√3	± (11) ± (1-2) ± (2-1)
0.12	3.47	3.48	√4	± (20) ± (02) ± (2-2)
0.10	5.21	5.22	√9	± (30) ± (03) ± (3-3)

In the case of complex **4b** we could go deeper in our crystallographic study and deduce the charge-density map of the structure. For charge-density determination, we have to consider the intensity of the different reflections apart from their angular positions. The procedure is essentially an inverse Fourier transform of the diffraction diagram, and it can be carried out if the structure factors are real, which in practice holds for the symmetry of most mesophases. Assuming that this is the case, their absolute values are the square root of the intensities, and only their signs have to be determined. The correct sign combination is decided by the physical merit of the density map obtained, taking into account the packing conditions, molecular sizes and optimization of the steric interactions. The technical details of the procedure can be found in ref. 69.

Table 4. Small-angle reflections for **4b**. Peaks were indexed according to a hexagonal lattice with cell parameter a = 78 Å. All combinations of signs in the Miller indices are possible and correspond to symmetry equivalent reflections.

Reflec. No.	2θ (°) (exp.)	2θ (°) (calcd.)	Ratio of spacings d(10)/d(*hk*)	Miller indices (*hk*)
1	1.31	1.31	1	± (10) ± (01) ± (1-1)
2	2.28	2.26	√3	± (11) ± (1-2) ± (2-1)
3	3.37	3.46	√7	± (12) ± (2-3) ± (3-1) ± (21) ± (3-2) ± (1-3)
4	3.89	3.91	√9	± (30) ± (03) ± (3-3)
5	4.67	4.70	√13	± (13) ± (4-1) ± (3-4) ± (31) ± (1-4) ± (4-3)
6	5.74	5.69	√19	± (23) ± (5-2) ± (3-5) ± (32) ± (2-5) ± (5-3)
7	6.87	6.91	√28	± (24) ± (6-2) ± (4-6) ± (42) ± (2-6) ± (6-4)

Once corrections from the Lorentz and polarization factors were made, the four reflections with the highest intensities (see peaks Nos. 2, 3, 4, and 5 in Figure 4a) were considered. The resulting map is shown in Figure 5a and was chosen among the possible 2^4 maps. The brightest areas correspond to the highest electron density. The plane group is *p6mm*, which is the maximal hexagonal plane symmetry. We interpret the columns as formed by the stacking of strata of three molecules arranged of layers constituted by a molecular arrangement as indicated in Figure 5b. The V=O groups are located in the central region of the columns. Six triphenylene groups (two per molecule) are connected to the central part, and are also stacked in columns. Triphenylene groups of each stratum can overlap with any of those of the neighboring strata. V=O groups can interact with each other between consecutive strata. If the interaction were strong enough this could give rise to magnetic order with magnetization along the column axis. The distance between triphenylene and V=O groups is about 25 Å, in agreement with the calculations (ACD Laboratories Chemsketch). The calculated mass density is ρ = 0.8 g/cm^3.

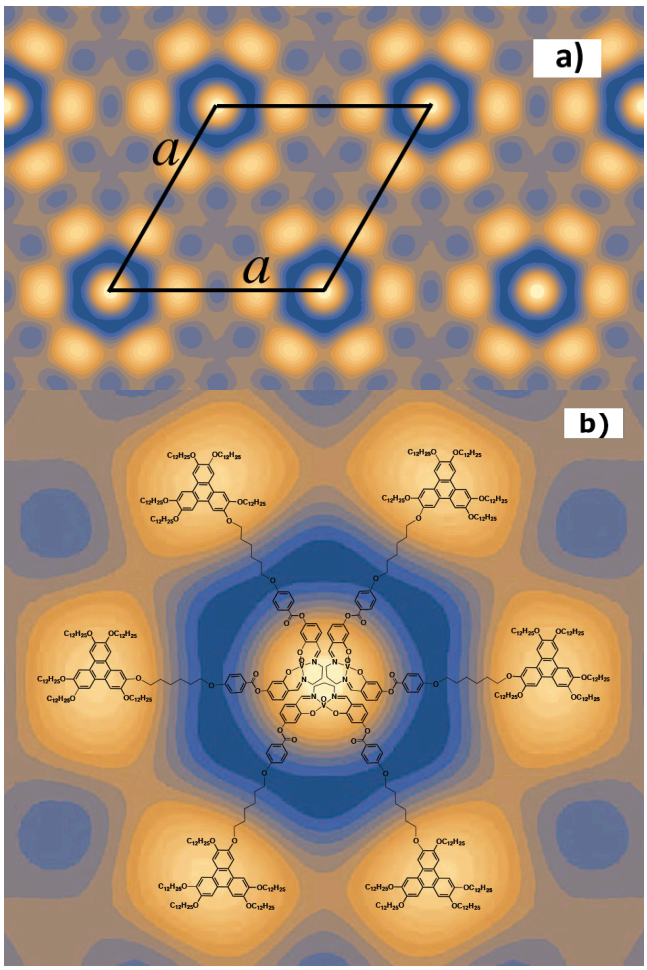

Figure 5. (**a**) Charge-density map deduced from the X-ray measurements of compound **4b**. The unit cell parameters are also sketched. The scale of the plot is deduced from the hexagonal cell parameter a =78 Å. (**b**) Organization of the molecules within the mesophase giving rise to a disc-like object with a charge density in accordance with (**a**). This object,

formed by three molecules, is the repeating unit whose stacking is the origin of the columns in the columnar mesophase.

Three-molecule objects like the one of Figure 5b form a column by stacking themselves, with the only restriction that triphenylene groups of each stratum overlap with those of the neighboring strata. Two stacking possibilities differing by a 60° rotation about the column axis can take place.

In a real liquid crystal phase disorder should exist and the molecular arrangement should be slightly displaced or rotated at random about the column axis. Therefore, the proposed molecular organization within the columns should be considered only as an idealized model. However, it is well supported that the structure of this mesophase contains segregated organic and inorganic columns, an arrangement favored by π-π stacking of triphenylene discs, and by the V=O→V=O interactions.

Electrochemical and Charge Mobility Studies.

In order to analyze the charge transport of these organometallic materials in mesophase, cyclic voltammetry experiments and hole mobility (μ) studies were performed for **1a**, and for **2a**, **3a** and **4b** as representative complexes. The cyclic voltammetry data are collected in Table 5.

Table 5. Electrochemical parameters (HOMO and LUMO energy levels).

Comp.	$E_{1/2}^{ox}$ (V)/eV[a]	E_{HOMO}/eV[b]	E_{LUMO}/eV[c]	Optical gap (E_g)/eV[d]
1a	0.951	-5.326	-2.026	3.300[e]
2a	0.936[*]	-5.294[*]	-2.051[e]	3.243[e]
			-2.695[f]	2.599[f]
3a	0.954[*]	-5.315[*]	-2.238[e]	3.077[e]
			-3.469[f]	1.846[f]
4b	0.946[e]	-5.317[e]	-2.249[e]	3.068[e]
	0.688[f]	-5.060[f]	-3.187[f]	1.873[f]

[a] V vs. calomel electrode with a platinum work electrode in dichloromethane. [b] E_{HOMO} (eV) = -[$E_{1/2}$ox(V)- $E_{1/2}$ox fc (V)] - 4.8(eV) ($E_{1/2}$ox fc is the averaged oxidation potential of the system ferrocene/ferricinium (Fc) versus the calomel electrode).[70] [c] LUMO potential were calculated from the optical gap observed in the absorption spectra and the HOMO potentials obtained with CV. [d] Optical gap calculated from E_g = 1242/λ_{onset} where λ_{onset} is the onset of the band of the absorption spectra that appears at highest wavelength. [e] Data from the triphenylene group. [f] Data from the metal moiety.[*] Redox process of triphenylene core and metal moiety overlapped.

The cyclic voltammograms were recorded in CH_2Cl_2 solution of tetra-n-butylammonium hexafluorophosphate (0.1 M). One oxidation wave was observed in all cases (Figure 6) at very similar potential (in the range 0.936–0.954 V) , corresponding to the triphenylene moieties.[49] The characteristic oxidation process $M^{n+}/M^{(n+1)+}$ of the metal-Salen fragments, expected to appear in the range 0.4-0.7 V for the vanadyl complexes,[71] and at about 0.9 V for the nickel[72,73] and copper[74] complexes, is clearly observed for the vanadyl complex at *ca*. 0.688 V. It is a reversible process, partially overlapped with that of the triphenylene (Figure 6 up). In the case of the copper and nickel complexes, the cyclic voltammetry wave of the triphenylene groups and that of the corresponding metal fragment were practically coincident, and only the overlapped wave is observed (Figures 6 bottom and figures S43-S45). This overlapping was confirmed recording cyclic voltammograms of the mixtures of the corresponding N,N'-ethylenedisalicyldeneaminate (Salen) copper, nickel and vanadyl complex with 2,3,6,7,10,11-hexadodecyloxytriphenylene in a 1:2 molar ratio (Figures S47-S49). An additional circumstance contributing to the non-observation of the expected metal contributions to the voltammograms is that the real concentration of the metal group at the electrode interface is probably low, as the metal fragment in the triphenylene complexes is surrounded by two triphenylene groups and ten dodecyloxy chains and the charge transfer process involving the metal fragment is diffusion controlled.[72]. Consequently, the expected intensity of these redox waves should be lower than for the homologous metal derivatives without triphenylene substituents, as observed for the vanadyl complex.

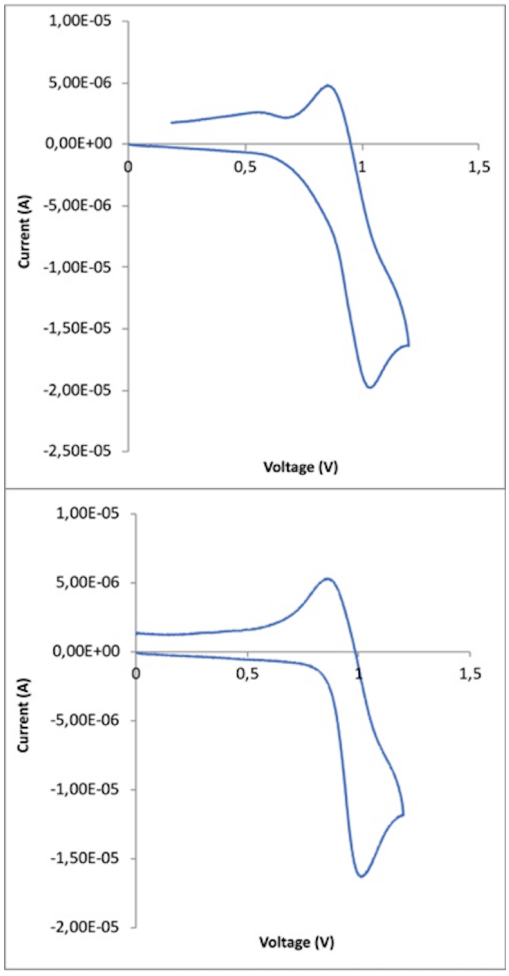

Figure 6. Cyclic voltammograms of **2a** (bottom) and **4b** (up).

In summary, the non-observation of the expected CV band for the Ni and Cu complexes is not in contradiction with the presence, as observed for vanadyl, of two conducting regions, the triphenylene columns and the columns of the metal moieties not electronically connected and constituting two independent electronic systems with their own HOMO, LUMO and gap values for each metal moiety (Table 5).

The hole mobility of the Schiff base **1a**, which is the only free ligand exhibiting a mesophase, and compounds **2a**, **3a** and **4b**, as representative of the metal complexes, was studied by the Space-Charge Limited Current (SCLC) method. The details of sample preparation and measurements are reported in the Supporting Information. Suitable results from SCLC measurements require an ohmic contact between the active material and the injecting electrode. In the case of hole conductors, this requirement is fulfilled using gold electrodes whose work-function matches the HOMO level energy of all compounds listed in Table 5.

The lack of crystalline order that usually characterizes amorphous or polycrystalline organic semiconductors leads to low values of charge mobility. The unidirectional order characteristic of columnar mesophases represents one of the most efficient ways to overcome this undesired limitation. When mobility is measured via SCLC or other techniques probing transport over long-range distances, in order to measure values representative of the real charge flow through columns, it is necessary to obtain homogeneous alignment of the columns between the electrodes. If polydomain morphology is present instead, the charge flow is suppressed at grain boundaries and much lower values of mobility are measured. The desired macroscopic orientation, in the geometry of our cells a homeotropic alignment, is spontaneously present in the N phase of complex **2a**, as shown in Figure 2b, and also, although to a lower extent, in the columnar phases formed by complexes **3a** and **4b**. In contrast, for ligand **1a**, a homogeneous macroscopic orientation was never achieved: as observed by POM, even after repeated thermal treatments, the morphology of the samples was always very far from a homogeneous homeotropic alignment.

The highest hole mobility value measured after several thermal treatments for the Salen ligand **1a** was of the order of 10^{-7} $cm^2 V^{-1} s^{-1}$. However, this low value may very well be a consequence of the polydomain morphology and it may not reflect the real features of charge flow through the triphenylene columns in the Col_h phase of **1a** (Table 6). In contrast, the values measured for the three complexes are the same within experimental error, in the order of 5 – 10 $cm^2 V^{-1} s^{-1}$. It is worth noting that the highest values measured on purely organic triphenylene columnar mesogens are in the range 10^{-3} – 10^{-1} $cm^2 V^{-1} s^{-1}$.[4] The values reported here for the three metal complexes are then 10-100 times higher than for well oriented organic triphenylene samples. As the decreased dynamic disorder (hindered rotations around the columnar axis), expected in our case for a discotic "dimer", is known not to induce such high values of charge mobility in triphenylene based systems,[75] a plausible explanation for the high mobility values obtained is a direct involvement of the metal-containing columns in hole transport.

Table 6. Hole mobility in compounds **1a**, **2a**, **3a**, **4b**.

Compound	Hole mobility ($cm^2 V^{-1} s^{-1}$)
1a	$3\pm 2.5\ 10^{-7*}$
2a	6 ± 5
3a	10 ± 5
4b	8 ± 5

* Polydomain morphology

In summary, the metal moieties play a double role in the remarkable hole mobility of these mesophases: they induce a longer length-scale of homogeneous orientational order (i.e. they reduce the tendency to form polydomains) and, more important, they also create their own columnar regions. Considering that the metal complex arrangement constitutes an independent electronic system, we suggest that the increase in the hole mobility in the metal complexes is due to the contribution of the inorganic regions. Finally, the fact that the same mobility was measured in a nematic phase (**2a**) as in columnar phases (**3a**, **4b**) should not be a surprise. Not only, as shown above by SAXS, the nematic phase of **2a** contains columnar units, but also hole mobilities of the same order of magnitude were recently reported for nematic phases formed by disk-shaped porphyrin dendrimers.[76] Incidentally, also in that case, high mobilities were measured only for metal-containing porphyrins.

CONCLUSIONS

In conclusion, we have prepared semiconducting organic and metal-organic nematic and columnar mesophases based on triphenylene Schiff-base derivatives. Their properties are modulated by the nature of the metallic group. The greater tendency of the Schiff-base complexes to self-assemble into inorganic linear structures, particularly through reasonably strong interactions (as with vanadyl), favors the formation of columnar mesophases, whereas a higher tendency to form discrete dimers as in Ni(Salen synton) stabilizes a nematic phase. In these systems, where the triphenylene core and the metal complex constitute two independent electronic systems, metal coordination reduces the tendency to form polydomain morphologies. In addition, in the columnar phases triphenylene cores and the metal complexes segregate in different columnar units. One likely explanation for the extraordinary enhancement of charge mobility observed in these metalorganic fluid systems, compared to the lower mobility in their purely organic precursors, is charge transport along the columns containing the metal fragment. Charge mobility evaluations are known to be sensitive to the experimental technique and for this reason a confirmation through a different measurement method would be desirable. However, the high hole mobility values achieved so far (of the order of 5 $cm^2 V^{-1} s^{-1}$) reveal a great potential of metalorganic triphenylene molecules as semiconducting soft materials suitable for applications in modern devices.

ASSOCIATED CONTENT

Supporting Information

Materials and methods. Full details of synthetic methods, spectroscopic data and analytical data for the new compounds. ^{1}H, and $^{13}C\{^{1}H\}$ NMR spectra of all new compounds. MALDI-TOF mass spectra. Details of hole mobility measurements.

The Supporting Information is available free of charge via the Internet at http://pubs.acs.org."

AUTHOR INFORMATION

Corresponding Author

* (S.C.) E-mail: scoco@qi.uva.es

* (P.E.) E-mail: espinet@qi.uva.es

‡These authors contributed equally. (match statement to author names with a symbol)

Author Contributions

The manuscript was written through contributions of all authors. / All authors have given approval to the final version of the manuscript. /

ACKNOWLEDGMENT

This work was sponsored by the Ministerio de Ciencia e Innovación (Project CTQ2017-89217-P), the Junta de Castilla y León (Project VA038G18), and the UPV/EHU (Project GIU18/146). E. D. thanks MECD for a FPU grant. R.T. was supported by the MERAVIGLIE project (CUP J28C17000080006).

REFERENCES

[1] Kumar, S. Self-organization of disc-like molecules: chemical aspects. *Chem. Soc. Rev*. **2006**, *35*, 83−109.

[2] Kumar, S. Recent developments in the chemistry of triphenylene-based discotic liquid crystals. *Liq. Cryst.* **2004**, *31*, 1037−1059.

[3] Kumar, S.; Setia, S.; Avinash, B. S.; Kumar, S. Triphenylene-based discotic liquid crystals: recent advances. *Liq.Cryst.* **2013**, *40*, 1769−1816

[4] Wöhrle, T.; Wurzbach, I.; Kirres, J.; Kostidou, A.; Kapernaum, N.; Litterscheidt, J.; Haenle, J. H.; Staffeld, P.; Baro, A.; Giesselmann, F.; Laschat, S. Discotic liquid crystals. *Chem. Rev.* **2016**, *116*, 1139−1241.

[5] Adam, D.; Schuhmacher, P.; Simmerer, J.; Haussling, L.; Siemensmeyer, K.; Etzbachi, K. H.; Ringsdorf, H; Haarer, D. Fast photoconduction in the highly ordered columnar phase of a discotic liquid cristal. *Nature* **1994**, *371*, 141−143.

[6] Zhang, L.; Hughes, D. L.; Cammidge, A. N. Discotic Triphenylene Twins Linked through Thiophene Bridges: Controlling Nematic Behavior in an Intriguing Class of Functional Organic Materials. *J. Org. Chem*. **2012**, *77*, 4288−4297.

[7] Gupta, M; Pal, S. K. Triphenylene-Based Room-Temperature Discotic Liquid Crystals: A New Class of Blue-Light-Emitting Materials with Long-Range Columnar Self-Assembly. *Langmuir* **2016**, *32*, 1120−1126

[8] Bhalla, V.; Singh, H.; Kumar, M.; Prasad, S. K. Triazole-Modified Triphenylene Derivative: Self-Assembly and Sensing Applications. *Langmuir* **2011**, *27*, 15275−15281.

[9] Mansueto, M.; Sauer, S.; Butschies, M.; Kaller, M.; Baro, A.; Woerner, R.; Hansen, N. H.; Tovar, G.; Pflaum, J.; Laschat, S. Triphenylene Silanes for Direct Surface Anchoring in Binary Mixed Self-Assembled Monolayers. *Langmuir* **2012**, *28*, 8399−8407.

[10] Shen, Z.; Yamada, M.; Miyake, M. Control of Stripelike and Hexagonal Self-Assembly of Gold Nanoparticles by the Tuning of Interactions between Triphenylene Ligands. *J. Am. Chem. Soc*. **2007**, *129*, 14271−14280.

[11] Gowda, A.; Kumar, S. Recent Advances in Discotic Liquid Crystal-Assisted Nanoparticles. *Materials* **2018**, *11*, 382.

[12] Takeda, T.; Wu, J.; Ikenaka, N.; Hoshino, N.; Hisaki, I.; Akutagawa, T. C_3 Symmetric Hexaphenyltriphenylenehexamide: Molecular Design of Fluorescent Ferroelectrics. *ChemistrySelect* **2018**, *3*, 10608–10614.

[13] Mori, H.; Itoh, Y.; Nishiura, Y.; Nakamura, T.; Shinagawa, Y. Performance of a novel optical compensation film ased on negative birefringence of discotic compound for wide-viewing-angle twisted-nematic liquid-crystal displays. *Jpn. J. Appl. Phys.* **1997**, *36*, 143−147.

[14] Boden, N.; Bushby, R. J.; Cammidge, A. N. Functionalization of discotic liquid crystals by direct substitution into the discogen ring: α-nitration of triphenylene-based discogens. *Liq. Cryst.* **1995**, *18*, 673−676.

[15] Boden, N.; Bushby, R. J.; Cammidge, A. N.; Headdock, G. Novel discotic liquid crystals created by electrophilic aromatic substitution. *J. Mater. Chem*. **1995**, *5*, 2275−2281.

[16] Kumar, S.; Manickam, M.; Balagurusamy, V. S. K.; Schonherr, H. Electrophilic aromatic substitution in triphenylene discotics: synthesis of alkoxynitrotriphenylenes *Liq. Cryst*. **1999**, *26*, 1455−1466.

[17] Bushby, R. J.; Boden, N.; Kilner, C. A.; Lozman, O. R.; Lu, Z.; Liu, Q.; Thornton-Pett, M. A. Helical geometry and liquid crystalline properties of 2,3,6,7,10,11-hexaalkoxy-1-nitrotriphenylenes. *J. Mater. Chem*. **2003**, *13*, 470–474.

[18] Boden, N.; Bushby, R. J.; Lu, Z. B.; Cammidge, A. N. Cyano substituted triphenylene-based discotic mesogens. *Liq. Cryst*. **1999**, *26*, 495−499.

[19] Praefcke, K.; Eckert, A.; Blunk, D. Liquid crystalline compounds. Part 105. Core-halogenated, helical-chiral triphenylene-based columnar liquid crystals. *Liq. Cryst.* **1997**, *22*, 113−119.

[20] Boden, N.; Bushby, R. J.; Cammidge, A. N.; Duckworth, S.; Headdock, G. α-Halogenation of triphenylene-based discotic liquid crystals: towards a chiral nucleus. *J. Mater. Chem*. **1997**, *7*, 601−605.

[21] Boden, N.; Bushby, R. J.; Cammidge, A. N.; Headdock, G. Versatile synthesis of unsymmetrically substituted triphenylenes. *Synthesis* **1995**, 31−32.

[22] Kumar, S.; Manickam, M.; Varshney, S. K.; Rao, D. S. S.; Prasad, S. K. Novel heptasubstituted triphenylene discotic liquid crystals. *J. Mater. Chem*. **2000**, *10*, 2483−2489.

[23] Kumar, S.; Varshney, S. K. A new form of discotic metallomesogens: the synthesis of metal-bridged triphenylene discotic dimers. *Liq. Cryst.* **2001**, *28*, 161−163.

[24] Schulte, J. L.; Laschat, S.; Schulte-Ladbeck, R.; von Arnim, V.; Schneider, A.; Finkelmann, H. Preparation of (η^6-alkoxytriphenylene)tricarbonyl chromium(0) complexes: Mesomorphic properties of a disk-shaped chromium–arene complex. *J. Organomet. Chem.* **1998**, *552*, 171−176.

[25] Cammidge, A. N.; Gopee, H. Macrodiscotic triphenylenophthalocyanines. *Chem. Comm.* **2002**, 966−967.

[26] Mohr, B.; Wegner, G.; Ohta, K. Synthesis of triphenylene-based porphyrazinato metal(II) complexes which display discotic columnar mesomorphism. *Chem. Comm.* **1995**, 995−996.

[27] Yang, F.; Bai, X.; Guo, H.; Li, C. Ion complexation-induced mesomorphic conversion between two columnar phases of novel symmetrical triads of triphenylene-calix[4]arene-triphenylenes. *Tetrahedron Lett.* **2013**, *54*, 409−413.

[28] Shi, J.; Wang, Y.; Xiao, M.; Zhong, P.; Liu, Y.; Tan, H.; Zhu, M.; Zhu, W. Luminescent metallomesogens based on platinum complex containing triphenylene unit. *Tetrahedron* **2015**, *71*, 463−469.

[29] Chico, R.; Domínguez, C.; Donnio, B.; Heinrich, B.; Coco, S.; Espinet, P. Isocyano-Triphenylene Complexes of Gold, Copper, Silver, and Platinum. Coordination Features and Mesomorphic Behavior. *Cryst. Growth Des*. **2016**, *16*, 6984−6991.

[30] Kumar, S. Triphenylene-based discotic liquid crystal dimers, oligomers and polymers**.** *Liq. Cryst.* **2005**, *32*, 1089−1113.

[31] Beltrán, E.; Garzoni, M.; Feringán, B.; Vancheri, A.; Barberá, J.; Serrano, J. L.; Pavan, G. M.; Giménez, R.; Sierra, T. Self-organization of star-shaped columnar liquid crystals with a coaxial nanophase segregation revealed by a combined experimental and simulation approach. *Chem. Commun*. **2015**, *51*, 1811−1814.

[32]Xiao, Y.; Su, X.; Sosa-Vargas, L.; Lacaze, E.; Heinrich, B.; Donnio, B.; Kreher, D.; Mathevet, F.; Attias, A.-J. Chemical engineering of donor–acceptor liquid crystalline dyads and triads for the controlled nanostructuration of organic semiconductors. *CrystEngComm.* **2016**, *18* ,4787–4798.

[33] Gupta, S. P.; Gupta, M.; Pal, S. K. Highly Resolved Morphology of Room-Temperature Columnar Liquid Crystals Derived from Triphenylene and Multialkynylbenzene Using Reconstructed Electron Density Maps. *ChemistrySelect* **2017**, *2*, 6070–6077.

[34] Feringán, B.; Romero, P.; Serrano, J. L.; Folcia, C. L.; Etxebarria, J.; Ortega, J.; Termine, R.; Golemme, A.; Giménez, R.; Sierra, T. H-Bonded Donor–Acceptor Units Segregated in Coaxial Columnar Assemblies: Toward High Mobility Ambipolar Organic Semiconductors. Segregated Donor–Acceptor Columns in Liquid Crystals That Exhibit Highly Efficient Ambipolar Charge Transport. *J. Am. Chem. Soc*. **2016**, *138*, 12511−12518.

[35] Hayashi, H.; Nihashi, W.; Umeyama, T.; Matano, Y.; Seki, S.; Shimizu, Y.; Imahori, H. Segregated Donor–Acceptor Columns in Liquid Crystals That Exhibit Highly Efficient Ambipolar Charge Transport. *J. Am. Chem. Soc*. **2011**, *133*, 10736−10739.

[36] Xiao, Y.; Su, X.; Sosa-Vargas, L.; Lacaze, E.; Heinrich, B.; Donnio, B.; Kreher, D.; Mathevet, F.; Attias, A. J. Chemical engineering of donor–acceptor liquid crystalline dyads and triads for the controlled nanostructuration of organic semiconductors. *Cryst. Eng. Comm.* **2016**, *18*, 4787–4798.

[37] Zhao, K.-Q.; An, L.-L.; Zhang, X.-B.; Yu, W.-H.; Hu, P.; Wang, B.-Q.; Xu, J.; Zeng, Q.-D.; Monobe, H.; Shimizu, Y.; Heinrich, B.; Donnio, B. Highly Segregated Lamello-Columnar Mesophase Organizations and Fast Charge Carrier Mobility in New Discotic Donor–Acceptor Triads. *Chem. Eur. J.* **2015**, *21*, 10379-10390.

[38] Kira, A.; Umeyama, T.; Matano, Y.; Yoshida, K.; Isoda, S.; Park, J. K.; Kim, D.; Imahori, H. Supramolecular Donor−Acceptor Heterojunctions by Vectorial Stepwise Assembly of Porphyrins and Coordination-Bonded Fullerene Arrays for Photocurrent Generation. *J. Am. Chem. Soc*. **2009**, *131*, 3198−3200.

[39] Umeyama, T.; Tezuka, N.; Kawashima, F.; Seki, S.; Matano, Y.; Nakao, Y.; Shishido, T.; Nishi, M.; Hirao, K.; Lehtivuori, H.; Tkachencko, N. V.; Lemmetyinen, H.; Imahori, H. Carbon Nanotube Wiring of Donor–Acceptor Nanograins by Self-Assembly and Efficient Charge Transport. *Angew. Chem., Int. Ed*. **2011**, *50*, 4615−4619.

[40] Tritto, E.; Chico, R.; Sanz-Enguita, G.; Folcia, C. L.; Ortega, J.; Coco, S.; Espinet, P. Alignment of Palladium Complexes into Columnar Liquid Crystals Driven by Peripheral Triphenylene Substituents. *Inorg. Chem.* **2014**, *53*, 3449−3455.

[41] Miguel-Coello, A. B.; Bardají, M.; Coco, S.; Donnio, B.; Heinrich, B.; Espinet, P. Triphenylene-Imidazolium Salts and Their NHC Metal Complexes, Materials with Segregated Multicolumnar Mesophases. *Inorg. Chem.* **2018**, *57*, 4359−4369.

[42] Tritto, E.; Chico, R.; Ortega, J.; Folcia, C. L.; Etxebarria, J.; Coco, S.; Espinet, P. Synergistic π–π and Pt–Pt interactions in luminescent hybrid inorganic/organic dual columnar liquid crystals. *J. Mater. Chem. C* **2015**, *3*, 9385−9392.

[43] Hegmann,T.; Kain, J.; Diele, S.; Schubert, B.; Bögel, H.; Tschierske, C. Molecular design at the calamitic/discotic cross-over point. Mononuclear ortho-metallated mesogens based on the combination of rod-like phenylpyrimidines and -pyridines with bent or half-disc-shaped diketonates. *J. Mater. Chem*. **2003**, *13*, 991–1003.

[44] Kozhevnikov, V. N.; Donnio, B.; Bruce, D. W. Phosphorescent, Terdentate, Liquid-Crystalline Complexes of Platinum(II): Stimulus-Dependent Emission. *Angew. Chem. Int. Ed.* **2008**, *47*, 6286 –6289.

[45] Wang, Y.; Liu, Y.; Luo, J.; Qi, H.; Li, X.; Nin, M.; Liu, M.; Shi, D.; Zhu, W.; Cao, Y. Metallomesogens based on platinum(II) com plexes: synthesis, luminescence and polarized emission. *Dalton Trans*. **2011**, *40*, 5046–5051.

[46] Wu, X.; Zhu, M.; Bruce, D. W.; Zhu, W.; Wang, Y. An over view of phosphorescent metallomesogens based on platinum and iridium. *J. Mater. Chem. C*, **2018**, *6*, 9848−9860.

[47] Bachman, R. E.; Fioritto, M. S.; Fetics, S. K.; Cocker, T. M. The Structural and Functional Equivalence of Aurophilic and Hydrogen Bonding: Evidence for the First Examples of Rotator Phases Induced by Aurophilic Bonding. *J. Am. Chem. Soc*. **2001**, *123*, 5376-5377.

[48] Coco, S.; Cordovilla, C.; Espinet, P.; Martín-Álvarez, J.; Muñoz, P. Dinuclear Gold(I) Isocyanide Complexes with Luminescent Properties, and Displaying Thermotropic Liquid Crystalline Behavior. *Inorg. Chem*. **2006**, *45,* 10180−10187.

[49] Chico, R.; de Domingo, E.; Domínguez, C.; Donnio, B.; Heinrich, B.; Termine, R.; Golemme, A.; Coco, S.; Espinet, P. High One-Dimensional Charge Mobility in Semiconducting Columnar Mesophases of Isocyano-Triphenylene Metal Complexes. *Chem. Mater*. **2017**, *29*, 7587−7595.

[50] *Metallomesogens*; Serrano, J. L., Ed.; VCH: Weinheim, 1996.

[51] Donnio, B.; Guillon, D.; Bruce, D. W.; Deschenaux, R. Metallomesogens. In *Comprehensive Organometallic Chemistry III: From Fundamentals to Applications*; Crabtree, R. H., Mingos, D. M. P., Eds.; Elsevier: Oxford, U.K., 2006; Chapter 12.05, pp 195−294.

[52] Hoshino, N. Liquid crystal properties of metal-salicylaldimine complexes. Chemical modifications towards lower symmetry. *Coord. Chem. Rev.* **1998***, 174,* 77−108.

[53] Siegler, M. A.; Lutz, M. Ni(Salen): a System That Forms Many Solvates with Interacting Ni Atoms. *Cryst. Growth Des*. **2009**, *9,* 1194−1200.

[54] Singh, A. K.; Kumari, S.; Guru Row, T. N.; Prakash, J.; Kumar, K. R.; Sridhar, B.; Rao, T. R. Coordination of a mesogenic Schiff-base with Mn^{II}, Co^{II}, Ni^{II}, Cu^{II} and Zn^{II}: Synthesis, spectral studies and crystal structures. *Polyhedron* **2008**, *27*, 3710–3716.

[55] Serrette, A.; Carroll, P. J.; Swager, T. M. Tuning the intermolecular dative interactions in vanadium-oxo linear chain compounds: formation of a new type of liquid crystalline polymer. *J. Am. Chem. Soc.* **1992**, *114*, 1887−1889.

[56] Serrette, A. G.; Swager, T. M. Controlling intermolecular associations with molecular superstructure: polar discotic linear chain phsses. *J. Am. Chem. Soc.* **1993**, *115*, 8879−8880.

[57] Cano, M.; Oriol, L.; Pinol, M; Serrano, J. L. Photopolymerization of Reactive Mesogenic Schiff Bases and Related Metallomesogens. *Chem. Mater.* **1999**, *11*, 94−100.

[58] Hikmet, R. A. M.; Lub, J.; Tol, A. J. W. Effect of the Orientation of the Ester Bonds on the Properties of Three Isomeric Liquid Crystal

Diacrylates before and after Polymerization. *Macromolecules* **1995**, *28*, 3313−3327.

[59] Ros, M. B.; Ruiz, N.; Serrano, J. L.; Espinet, P. Metallomesogens based on ortho-palladated polar imines. III. Influence of the polar group position. *Liq. Cryst.* **1991**, *9*, 77–86.

[60] Orio, M.; Jarjayes, O.; Kanso, H.; Philouze, C.; Neese, F.; Thomas, F. X-Ray Structures of Copper(II) and Nickel(II) Radical Salen Complexes: The Preference of Galactose Oxidase for Copper(II). *Angew. Chem. Int. Ed.* **2010**, *49*, 4989–4992.

[61] Bezaatpour, A.; Behzad, M.; Boghaei, D. M. Synthesis, characterization and studies of mechanochemical, electrochemical, and thermal behavior of electronegative oxovanadium(IV) Schiff-base complexes. *J. Coord Chem*. **2009**, *62*, 1127–1133.

[62] Markovitsi, D.; Germain, A.; Millié, P.; Lécuyer, P.; Gallos, L. K.; Argyrakis, P.; Bengs, H.; Ringsdorf, H. Triphenylene Columnar Liquid Crystals: Excited States and Energy Transfer. *J. Phys. Chem.* **1995**, *99*, 1005−1017.

[63] Marguet, S.; Markovitsi, D.; Millié, P.; Sigal, H.; Kumar, S. Influence of Disorder on Electronic Excited States: An Experimental and Numerical Study of Alkylthiotriphenylene Columnar Phases. *J. Phys. Chem. B* **1998**, *102*, 4697−4710.

[64] Blackburn, O. A.; Coe, B. J.; Fielden, J.; Helliwell, M.; McDouall, J. J. W.; Hutchings, M. G. Nickel(II) and Palladium(II) Complexes of Azobenzene-Containing Ligands as Dichroic Dyes. *Inorg. Chem.* **2010**, *49*, 9136–9150.

[65] Greenbank, W. A.; McGrath, K. M. Photophysical behavior of 4-hexyloxysalicylaldimies and copper(II) complexes. *J. Photochem. Photobiol. A* **2014**, *279,* 52−58.

[66] Drew, M. G. B. Structure of (N,N'-Trimethyllenedisalicylideneaminato)nickel(II) (1) and (N,N'-Trimethyllenedisalicylideneaminato)copper(II) (2). *Acta Cryst.* **1985**, *C41*, 1755-1758.

[67] Zheng, H.; Lai, C. K.; Swager, T. M. Transition Metals in Highly Correlated Discotic Phases: Designing Metallomesogens with Selected Intermolecular Organizations. *Chem. Mater*. **1994**, *6*, 101−103.

[68] Serette, A. G., Swager, T. M. Polar Superstructures Stabilized by Polymeric Oxometal Units: Columnar Liquid Crystals Based on Tapered Dioxomolybdenum Complexes. *Angew. Chem., int. Ed. Engl*. **1994**, *33*, 2342−2345.

[69] Folcia, C. L.; Alonso, I.; Ortega, J.; Etxebarria, J.; Pintre, I.; Ros, M. B. Achiral Bent-Core Liquid Crystals with Azo and Azoxy Linkages: Structural and Nonlinear Optical Properties and Photoisomerization. *Chem. Mater*. **2006**, *18*, 4617−4626.

[70] Ahmida, M. M..; Eichhorn, S. H. Measurements and Prediction of Electronic Properties of Discotic Triphenylenes and Phthalocyanines. *ECS Trans*. **2010**, *25*, 1−10.

[71] A.H. Kianfar, A. H.; Mohebbi, S. Synthesis and Electrochemistry of Vanadium(IV) Schiff Base Complexes. *J. Iran. Chem. Soc*. **2007**, *4*, 215−220.

[72] Santos, I. C.; Vilas-Boas, M.; Piedade, M. F. M.; Freire C.; Duarte, M.T.; de Castro, B. Electrochemical and X-ray studies of nickel(II) Schiff base complexes derived from salicylaldehyde. Structural effects of bridge substituents on the stabilisation of the +3 oxidation state. *Polyhedron* **2000**, *19*, 655–664.

[73] Zolezzi, S.; Spodine, E.; Decinti, A. Electrochemical studies of copper(II) complexes with Schiff-base ligands. *Polyhedron* **2002**, *21*, 55–59.

[74]Benramdanea, R.; Benghanema,F.; Ouraria, A.; Keraghela, S.; Bouetb, G. Synthesis and characterization of a new Schiff base derived from 2,3 diaminopyridine and 5-methoxysalicylaldehyde and its Ni(II), Cu(II) and Zn(II) complexes. Electrochemical and electrocatalytical studies. *J. Coord. Chem.* **2015**, *68*, 560−572.

[75] Wang, J.; Zhang, C.; Zhang, S.; Hao, X.; Hong, F.; Zhang, A.; Wang, Y.-F.; Wu, H.; Zhang, W.; Pu, J.-L. A systematic study on the influences of linkage length on phase behaviours and charge carrier mobilities of discotic dimers. *Liq. Cryst.* **2017** *44*, 394-404.

[76] Concellón, A.; Marcos, M.; Romero, P.; Serrano, J. L.; Termine, R.; Golemme, A. Not Only Columns: High Hole Mobility in a Discotic Nematic Mesophase Formed by Metal-Containing Porphyrin-Core Dendrimers. *Angew. Chem. Int. Ed*. **2017**, *56*, 1259−1263.

TOC synopsis

The coordination of copper(II), nickel(II) or oxovanadium(IV) to triphenylene-Schiff-Base semiconducting mesophases produces a striking charge mobility enhancement of eight orders of magnitude along the columnar stacking, due to the contribution of the metal-containing columns.

TOC graphic